


RESEARCH ARTICLE



Design and synthesis of triazolopyridine derivatives as potent JAK/HDAC dual inhibitors with broad-spectrum antiproliferative activity

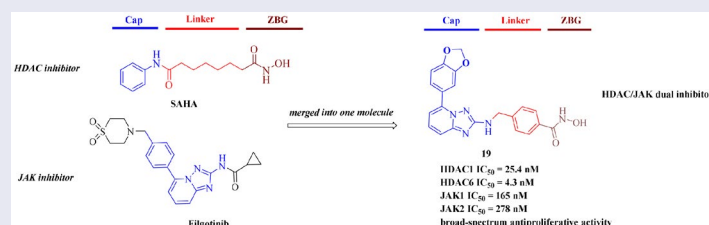
Zhengshui Xu^{a,b,†}, Changchun Ye^{c,†}, Xingjie Wang^c, Ranran Kong^a, Zilu Chen^{c,d}, Jing Shi^e, Xin Chen^f  and Shiyuan Liu^{a,b}

^aDepartment of Thoracic Surgery, The Second Affiliated Hospital of Xi'an Jiaotong University, Xi'an, Shaanxi, P. R. China; ^bKey Laboratory of Surgery Critical Care and Life Support, Ministry of Education, Xi'an Jiaotong University, Xi'an, Shaanxi, P. R. China; ^cDepartment of General Surgery, The First Affiliated Hospital of Xi'an Jiaotong University, Xi'an, Shaanxi, P. R. China; ^dRutgers Cancer Institute of New Jersey, New Brunswick, NJ, USA; ^eDepartment of Respiratory and Endocrinology, The Second Affiliated Hospital of Xi'an Jiaotong University, Xi'an, Shaanxi, P. R. China; ^fShaanxi Key Laboratory of Natural Products & Chemical Biology, College of Chemistry & Pharmacy, Northwest A&F University, Yangling, P. R. China

ABSTRACT

A series of triazolopyridine-based dual JAK/HDAC inhibitors were rationally designed and synthesised by merging different pharmacophores into one molecule. All triazolopyridine derivatives exhibited potent inhibitory activities against both targets and the best compound 4-(((5-(benzo[d][1,3]dioxol-5-yl)-[1,2,4]triazolo[1,5-a]pyridin-2-yl)amino)methyl)-N-hydroxybenzamide (19) was dug out. 19 was proved to be a pan-HDAC and JAK1/2 dual inhibitor and displayed high cytotoxicity against two cancer cell lines MDA-MB-231 and RPMI-8226 with IC₅₀ values in submicromolar range. Docking simulation revealed that 19 fitted well into the active sites of HDAC and JAK proteins. Moreover, 19 exhibited better metabolic stability in vitro than SAHA. Our study demonstrated that compound 19 was a promising candidate for further preclinical studies.

GRAPHICAL ABSTRACT



ARTICLE HISTORY

Received 23 July 2024
Revised 5 September 2024
Accepted 23 September 2024

KEYWORDS





HDAC; JAK; triazolopyridine; inhibitor; antiproliferative


Introduction

Histone deacetylases (HDACs), as promising targets for cancer therapy, control the acetylation levels of nuclear proteins and cytoplasmic proteins^{1–4}. The classical 11 zinc-dependent isoforms comprise class I (HDAC1, HDAC2, HDAC3, HDAC8), class IIa (HDAC4, 5, 7, 9), class IIb (HDAC6, 10), and class IV (HDAC11)^{5,6}. The anticarcinogenic mechanisms by the inhibition of HDACs generally included reduced cell motility/migration, invasion, induction of apoptosis, angiogenesis, and blocking of DNA repair. The pharmacophore of HDAC inhibitors (HDACis) have been well summarised: a capping motif occupying the outside of the protein's active pocket, a zinc-binding group (ZBG) such as hydroxamic acid or *ortho*-aminoaniline chelating the catalytically active zinc ion, and a

linker chain connecting the above two parts (Figure 1)^{7–11}. Such a pharmacophore model usually applies to all isoforms due to the highly conserved nature of HDAC family^{12–14}. Approved hydroxamic acid inhibitors including vorinostat (1, SAHA)¹⁵, belinostat (2)¹⁶, panobinostat (3)¹⁷ and natural romidepsin (5)¹⁸ have been used for the treatment of cutaneous T-cell lymphoma, peripheral T-cell lymphoma or multiple myeloma. Chidamide (4), an *ortho*-aminoaniline inhibitor, was approved for treating recurrent and refractory peripheral T-cell lymphoma by the China Food and Drug Administration in 2015¹⁹. Although a great success appeared in the discovery of new HDACis, the main challenge for HDAC-targeted clinical therapy is still the deficient efficacy against solid tumours²⁰.

A lot of literatures have described the synergistic and additive effects by the joint use of HDACis and kinases inhibitors^{21–24}.

CONTACT Xin Chen  chenxin1888@nwsuaf.edu.cn  Shaanxi Key Laboratory of Natural Products & Chemical Biology, College of Chemistry & Pharmacy, Northwest A&F University, Yangling, P. R. China; Shiyuan Liu  liushiyuan@xjtu.edu.cn  Department of Thoracic Surgery, The Second Affiliated Hospital of Xi'an Jiaotong University, Xi'an, Shaanxi, P. R. China

 Supplemental data for this article can be accessed online at <https://doi.org/10.1080/14756366.2024.2409771>.

[†]The authors contributed equally to this work.

© 2024 The Author(s). Published by Informa UK Limited, trading as Taylor & Francis Group
This is an Open Access article distributed under the terms of the Creative Commons Attribution-NonCommercial License (<http://creativecommons.org/licenses/by-nc/4.0/>), which permits unrestricted non-commercial use, distribution, and reproduction in any medium, provided the original work is properly cited. The terms on which this article has been published allow the posting of the Accepted Manuscript in a repository by the author(s) or with their consent.

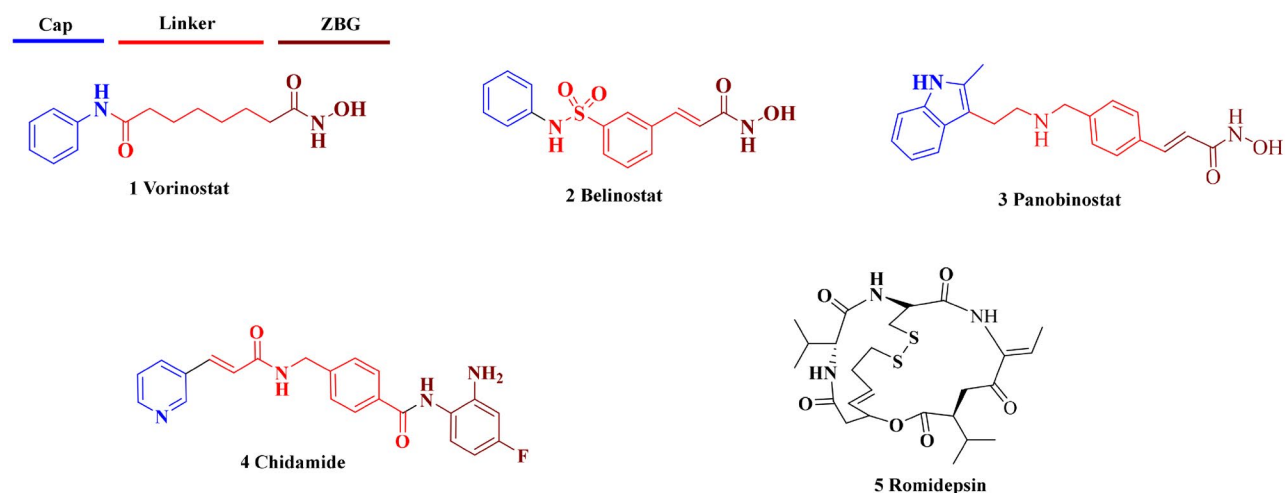


Figure 1. Approved HDAC inhibitors.

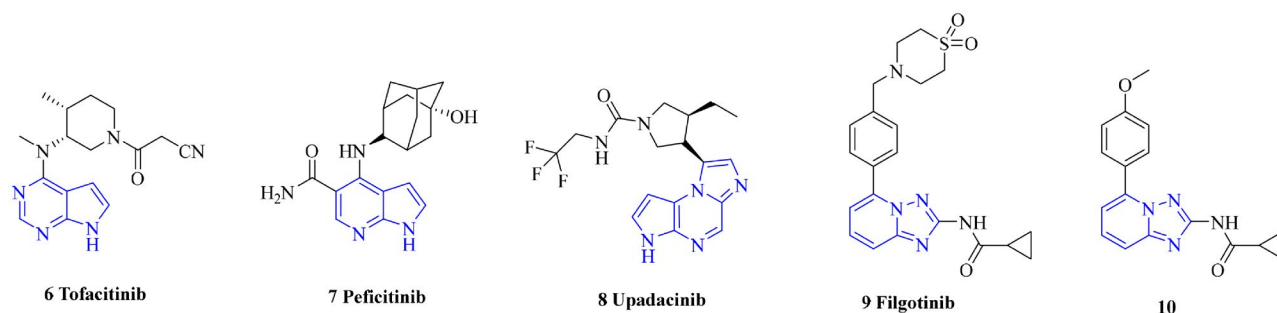


Figure 2. Representative JAK inhibitors.

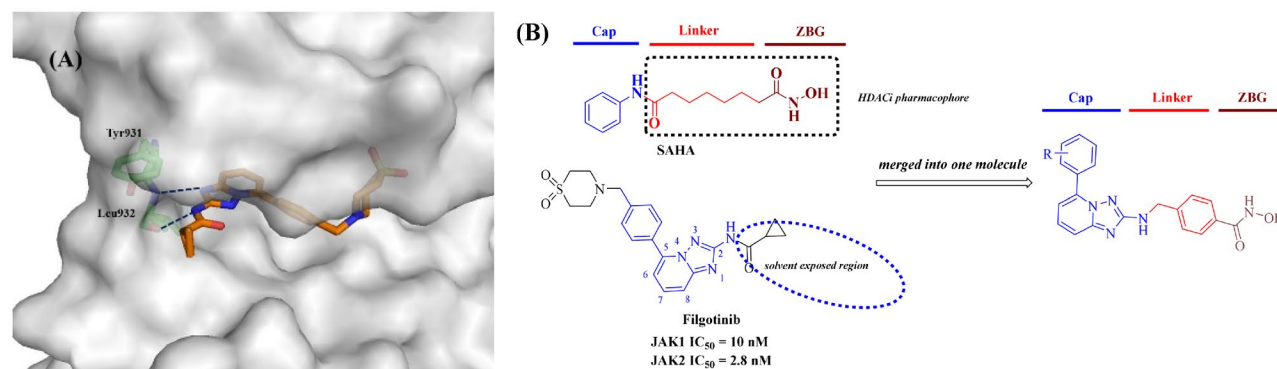
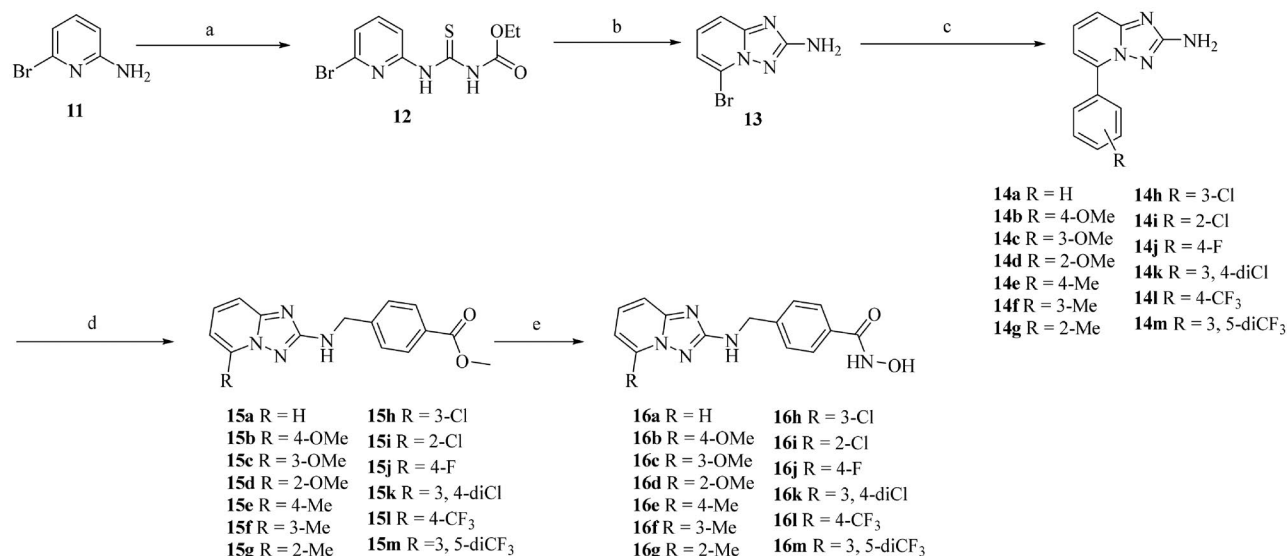


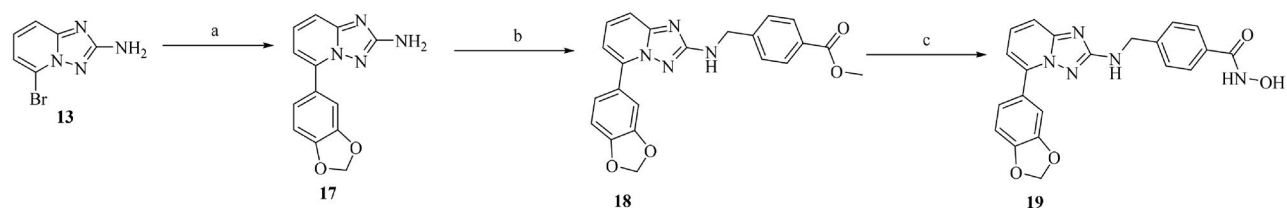
Figure 3. (A) Crystal structure of JAK2 with Filgotinib (PDB: 4P7E). (B) Design of triazolo-pyridines-based JAK/HDAC dual inhibitors.

Recently, several researchers revealed that combining Janus kinases (JAKs) and HDAC was expected to overcome the limitations of HDACis and bring clinical benefits to solid tumors^{25–28}. JAKs, composed of JAK1, JAK2, JAK3, and tyrosine kinase 2 (TYK2), are a family of intracellular tyrosine kinases that transduce cytokine-mediated signals through the JAK-STAT pathway^{29,30}. Inhibition of JAKs, especially JAK1 and JAK2, is a promising way to block the biological crosstalk between tumour cells and the surrounding cells in the tumour microenvironment^{31,32}. By so far, several JAK inhibitors have been approved for clinical use such as Tofacitinib (6)³³, Peficitinib (7)³⁴, Upadacitinib (8)³⁵, and Filgotinib (9)³⁶, as shown in Figure 2.

The common pharmacophore-based design strategy for multi-target drugs included conjugated-pharmacophore, fused-pharmacophore, and merged-pharmacophore^{37–39}. In this research, the rationale for the dual-inhibitor design originated from our sweeping investigations on reported X-ray crystal structure of Filgotinib bound to JAK2 (Figure 3(A))⁴⁰. One could appreciate several key interactions: triazolo-pyridine scaffold acted as an ATP mimetic and formed an important H-bond with Tyr931 residue. The adjacent amide also had an H-bond with Leu932 of the hinge region. The phenyl substituent on 5-position of the triazolo-pyridine scaffold probed into an internal crowded subpocket. While the cyclopropyl group of Filgotinib pointed towards an open space



Scheme 1. Reagents and conditions: (a) ethoxycarbonyl isothiocyanate, DCM, r.t. 16h; (b) hydroxylamine hydrochloride, DIPEA, EtOH/MeOH, reflux, 3 h; (c) various phenylboronic acids, Pd(dppf)Cl₂·K₂CO₃, 1, 4-dioxane/water, 100 °C, overnight; (d) methyl 4-formylbenzoate, MeOH, acetic acid, NaBH₃CN, 6 h, r.t.; (e) NH₂OH (aq), KOH, MeOH, 0 °C, 6 h.



Scheme 2. Reagents and conditions: (a) benzo[d][1,3]dioxol-5-ylboronic acid, Pd(dppf)Cl₂, K₂CO₃, 1, 4-dioxane/water, 100 °C, overnight; (b) methyl 4-formylbenzoate, MeOH, acetic acid, NaBH₃CN, 6 h, r.t.; (c) NH₂OH (aq), KOH, MeOH, 0 °C, 6 h.

(solvent-exposed region) that could possibly accommodate a relatively large motif. We envisioned that an appropriate linker and ZBG belonging to HDACi pharmacophore could be attached to 2-amino through the replacement of cyclopropylamide and the resulting compound would have structural features of both JAK/HDAC inhibitors (Figure 3(B)). To reduce oversized molecular weight of new merged structure and improve ligand efficiency for both targets, we also removed the thiomorpholine group on 5-phenyl-triazolopyridine of Filgotinib as exemplified by compound 10 (JAK1 IC₅₀ = 70 nM; JAK2 IC₅₀ = 138 nM)⁴⁰, although such a change might lead to a decreased activity for JAK. Here, we reported the synthesis, structure–activity relationship (SAR) study and antiproliferative evaluation of these merged triazolopyridine derivatives.

Chemistry

According to the reported SAR of triazolopyridines as JAK inhibitor⁴⁰, phenyl on 5-position of triazolopyridine was preferred and favourable. Hence, further structural exploration was performed to investigate the effect of different substituted phenyls on HDAC and JAK enzymes when hydroxamic acid group was linked to triazolopyridine fragment. As shown in Scheme 1, the key procedure to synthesise the target derivatives 16a-m was the construction of triazolopyridine skeleton from the commercially available 2-amino-6-bromo-pyridine (11). Ethoxycarbonyl isothiocyanate reacted with 11 to form the thiourea 12, which was then reacted with

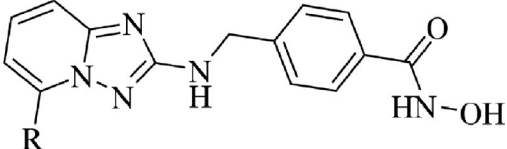
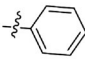
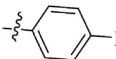
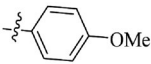
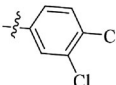
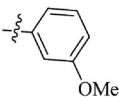
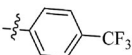
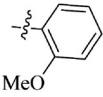
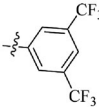
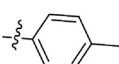
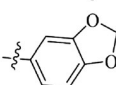
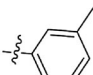
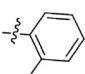
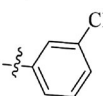
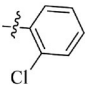
hydroxylamine to yield the desired intermediate 13 with *N,N*-diisopropylethylamine (DIPEA) as the base. Next, various phenylboronic acids were coupled to triazolopyridine scaffold via a Suzuki reaction to obtain intermediates 14a-m. Further reductive amination of 2-NH₂ on triazolopyridine core with methyl 4-formylbenzoate gave intermediates 15a-m, which upon treatment with an aqueous NH₂OH/NaOH solution provided hydroxamate analogues 16a-m. Compound 19 was synthesised in a similar way as exhibited in Scheme 2.

Results and discussion

JAK1, HDAC6 activities and SAR study of triazolopyridine derivatives

In our initial HDAC enzymatic screening, HDAC6 was chosen as the target protein because phenylhydroxamic acid was generally used in HDAC6 inhibitors¹⁰. All triazolopyridine derivatives were evaluated against JAK1 and HDAC6, with Filgotinib, SAHA and partially selective HDACi ACY-1215 as the positive compounds (Table 1). All compounds showed comfortable dual inhibition against JAK1 and HDAC6 with IC₅₀ in nanomolar range. 16b, a derivative of 10 in which its cyclopropylacetyl group was replaced with phenylhydroxamic acid exhibited excellent inhibitory activity against HDAC6 (IC₅₀ = 8.75 nM) and retained moderate inhibitory activity against JAK1 enzyme (IC₅₀ = 146 nM). While the methoxy group on 5-phenyl of triazolopyridine core was transferred to *ortho*- or *meta*-position,

Table 1. Initial evaluation of TH β C derivatives against JAK1 and HDAC6 (IC₅₀, nM)^a.

							
16a-m, 19							
Compound	R	JAK1	HDAC6	Compound	R	JAK1	HDAC6
16a		320 ± 18	9.50 ± 0.72	16j		295 ± 16	8.90 ± 0.16
16b		146 ± 8.5	8.75 ± 0.46	16k		390 ± 24	6.15 ± 0.12
16c		190 ± 10	8.40 ± 0.39	16l		460 ± 8.0	11.4 ± 0.88
16d		750 ± 30	10.2 ± 0.80	16m		685 ± 50	20.5 ± 0.78
16e		304 ± 16	11.0 ± 0.70	19		165 ± 13	4.30 ± 0.10
16f		315 ± 15	13.7 ± 0.88	10	/	72 ± 2.4	NA ^b
16g		550 ± 32	16.0 ± 1.1	Filgotinib	/	11.0 ± 0.32	/ ^c
16h		365 ± 25	9.65 ± 0.23	ACY-1215 ^c	/	/	5.13 ± 0.28
16i		400 ± 28	12.2 ± 0.30	SAHA	/	/	7.80 ± 0.57

^aWe ran experiments in duplicate, SD <15%. Assays were performed by Reaction Biology Corporation (Malvern, PA, USA). ^bNA: no activity. ^c: not tested.

Table 2. Complete characterisation of 19 at HDAC isoforms (IC₅₀^a, nM).

Cpd.	19	SAHA	Cpd.	19	SAHA
HDAC1	25.4 ± 1.20	4.37 ± 0.24	HDAC6	4.3 ± 0.09	7.80 ± 0.57
HDAC2	36.5 ± 0.95	12.1 ± 1.28	HDAC7	715 ± 33.5	> 50000
HDAC3	83.0 ± 2.40	3.34 ± 0.27	HDAC8	640 ± 28.3	1033 ± 62.5
HDAC4	> 50000	> 50000	HDAC11	1400 ± 102	895 ± 71.6
HDAC5	> 50000	> 50000			

^aWe ran experiments in duplicate, SD <15%. Assays were performed by Reaction Biology Corporation (Malvern, PA, USA).

Table 3. The screen of 19 against JAK isozymes (IC₅₀, nM).

Compound	IC ₅₀ a			
	JAK1	JAK2	JAK3	TYK2
19	165 ± 13	278 ± 20	> 10000	860 ± 33
Filgotinib	11.0 ± 0.32	28.6 ± 1.50	810 ± 45.0	116 ± 6.45

^aWe ran experiments in duplicate, SD <15%. Assays were performed by Reaction Biology Corporation (Malvern, PA, USA).

the resulting compounds 16c and 16d exhibited similar inhibitory activities against HDAC6, but both of them displayed less potent JAK1 activities, especially 16d. Removal of OMe (16a) also decreased

JAK1 inhibition. Compounds 16e-g with methyl substituent also showed a similar trend, but their HDAC6 activity were weaker. Besides, the introduction of electron-withdrawing groups such as chlorine (16i and 16k) or trifluoromethyl (16l and 16m) seemed to be detrimental to JAK1 activity but with no obvious influence on their HDAC6 activity. Compound 19 with a piperonyl showed the best potency against HDAC6 with IC₅₀ of 4.3 nM, better than those of SAHA and ACY-1215, and it also showed preferable JAK1 activity (IC₅₀ = 165 nM).

Compound 19 was further evaluated against HDAC or JAK isozymes to determine selectivity profile, and the result was shown in Table 2. 19 potently inhibited HDAC1 with an IC₅₀ of 25.4 nM, even though it was 6-fold weaker than HDAC6. 19 also showed inhibitory effect on HDAC2 and HDAC3 with IC₅₀ values of 36.5 nM (8.5-fold) and 83 nM (19-fold), respectively. Besides, much weaker inhibition of HDAC7, 8, 11 was observed. 19 showed no activity against HDAC4 and 5. On the other hand, 19 exhibited a mild but undifferentiated inhibitory activities against JAK1 and JAK2 with IC₅₀ values of 165 and 278 nM, respectively. However, 19 possessed very poor inhibitory activities against JAK3 and TYK2 (Table 3). This result establishes 19 to be a JAK1/2 inhibitor.

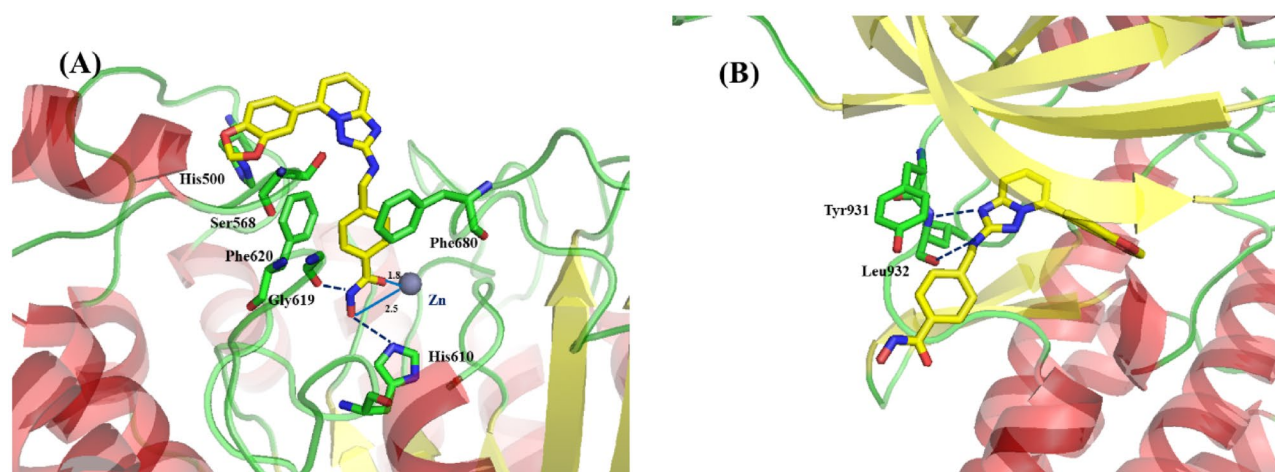


Figure 4. (A) Binding model of 19 (yellow) in the catalytic pocket of human HDAC6 (PDB code: 5EDU). (B) Binding model of 19 (yellow) in the catalytic pocket of JAK2 protein (PDB code: 4P7E). Key residues were labelled in green as sticks. Metal bonds and hydrogen bonds were labelled in baby blue and dark blue, respectively. Zinc ion was shown in brown.

Table 4. Antiproliferative effect of 16a-c, 16j and 19 against MDA-MB-231 and RPMI-8226 cell lines (IC_{50}^a , μM).

Compound	MDA-MB-231	RPMI-8226
16a	0.90 ± 0.03	0.46 ± 0.03
16b	0.84 ± 0.04	0.29 ± 0.01
16c	0.95 ± 0.02	0.31 ± 0.02
16j	0.88 ± 0.06	0.28 ± 0.06
19	0.75 ± 0.03	0.12 ± 0.01
Filgotinib	27.2 ± 1.5	17.5 ± 1.0
SAHA	5.40 ± 0.16	0.45 ± 0.01

^a IC_{50} values are averages of three independent experiments, SD <15%.

Molecular simulation

As shown in Figure 4(A), the docking results on 19 revealed that its hydroxamate group bound with Zn^{2+} in a bidentate manner. Besides, hydrogen bond interaction was formed between hydroxamic acid and Gly619 and His610. The model also suggested that the phenyl linker of 19 occupied the narrow tubular channel, making pi-interactions with both Phe620 and Phe680. The piperonyl of 19 occupied an external cleft created by His500 and Ser568 at the surface of HDAC6 protein. As seen in Figure 4(B), compound 19 showed a similar binding mode to that of Filgotinib in Figure 3. It also formed two key H-bonds with Tyr931 and Leu932 in the hinge region. The piperonyl of 19 was orthogonal to the triazolopyridine core and probed into a probably hydrophobic pocket in JAK2. And the phenylhydroxamic acid group pointed towards the solvent-exposed region as we expected. Such a binding mode matched well with the SAR of triazolopyridine derivatives in Table 1.

Antiproliferative evaluation

Compound 16a-c, 16j and 19 with preferred enzymatic inhibitory activity were selected to test their effects on tumour cell viability. As shown in Table 4, all five analogues showed potent and much better antiproliferative activity than the positive SAHA and Filgotinib, with IC_{50} values in submicromolar range. Multiple myeloma cell line RPMI-8226 was more sensitive to these triazolopyridines (IC_{50} , 0.1–0.46 μM) compared to breast cancer cell line MDA-MB-231 (IC_{50} , 0.7–0.95 μM). In particularly, a higher degree of distinction between these triazolopyridines and approved

SAHA against MDA-MB-231 cell line was observed, indicating their potential cellular potency against solid tumour cells. Among all, the best compound 19 potently inhibited MDA-MB-231 and RPMI-8226 cell lines with IC_{50} of 0.75 and 0.12 μM , respectively. In flow cytometry assay, 85.3% induction of RPMI-8226 cells apoptosis incubation with 1 μM of 19 was significantly higher than that of SAHA (62.2%) and Filgotinib (15.28%) at the same concentration (Figure 5).

Then, 19 was delivered to NCI-60 for the detailed examination of antitumor spectrum against different cancer cells include leukaemia, non-small cell lung cancer (NSCLC), colon cancer, CNS cancer, melanoma, ovary cancer, renal cancer, prostate cancer and breast cancer. According to Table 5, 19 displayed broad and potent nanomolar antiproliferative activity against almost all cancer cells. Three most sensitive cell lines were RPMI-8226, SR, HS 578T and NCI-H522 with GI_{50} values of 0.10 μM , 0.10 μM , 0.14 μM and 0.10 μM , respectively.

To further compare the sensitivity discrepancy of various cell lines to triazolopyridines, the mean log GI_{50} values of 19 for cell lines from the same type of cancer was calculated. The NCI-60 results of clinical ACY-1215 and SAHA were also listed as references, whose values could be obtained from https://dtp.cancer.gov/discovery_development/nci-60/ (original Log GI_{50} values were included in supporting information). On the basis of Figure 6, we observed that all mean GI_{50} values of 19 were significantly better than ACY-1215 and SAHA. Apart from leukaemia, 19 showed broad-spectrum anticancer effect against different solid tumours such as NSCLC, colon cancer, melanoma, ovary cancer, renal cancer, prostate cancer and breast cancer.

Microsomal stability study

Metabolic Stability of compound 19 was preliminary evaluated in human liver microsome (HLM) to determinate half-life ($T_{1/2}$). As shown in Table 6, the elimination $T_{1/2}$ values of 19 was 14.5 h in HLM, twice better than that of SAHA.

Conclusion

Co-inhibition of HDAC with JAK1/JAK2 was well established to be a synergistic way for treating solid tumours. In this paper, a series

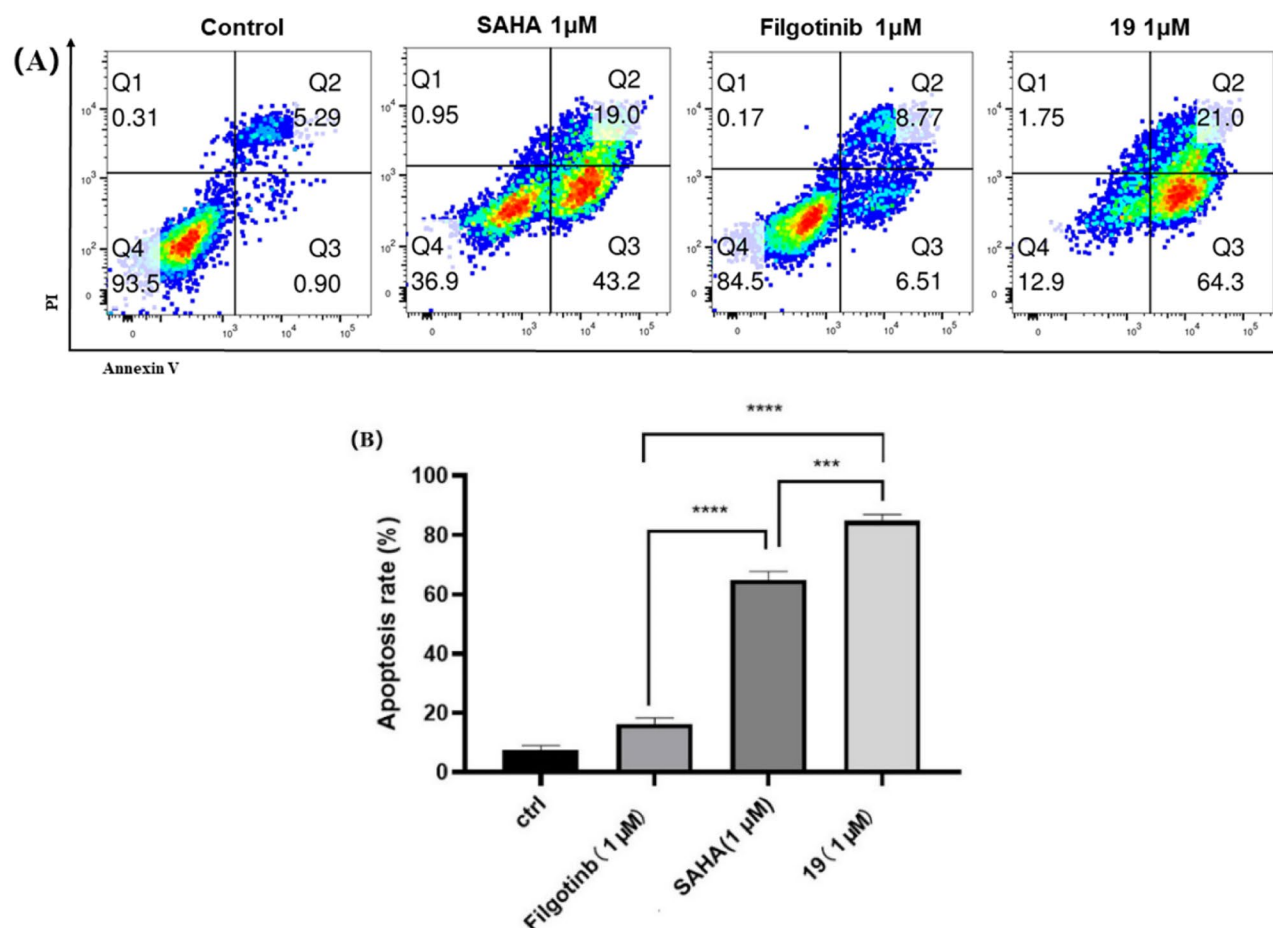


Figure 5. (A) Induction of apoptosis at 48h by compounds SAHA, Filgotinib and 19 at 1 μ M concentration in RPMI-8226 cell line by flow cytometry analysis. The percentage of cells in each part was indicated. (B) The histogram of filgotinib, SAHA and 19 on RPMI-8226 cells apoptosis. Data are the mean \pm SD of three independent experiments: *** p < 0.001 **** p < 0.0001 compared to the ctrl group.

Table 5. Antiproliferative screening against 59 cell lines of 19 (GI_{50} , μ M).

Cancer type	Cell line	19	Cancer type	Cell line	19
Leukaemia	CCRF-CEM	0.31	Non-Small Cell Lung Cancer	MALME-3M	0.25
	HL60	0.44		M14	0.55
	K-562	0.32		SK-MEL-2	0.25
	MOLT-4	0.35		SK-MEL-28	0.48
	RPMI-8226	0.10		SK-MEL-5	0.55
	SR	0.10		UACC-257	0.36
Non-Small Cell Lung Cancer	A549/ATCC	0.89	Ovarian Cancer	UACC-62	0.42
	EKVX	0.78		IGROV1	0.40
	HOP-62	/		OVCAR-3	0.42
	HOP-92	0.7		OVCAR-4	1.7
	NCI-H226	0.58		OVCAR-5	0.47
	NCI-H23	0.66		OVCAR-8	0.37
	NCI-H322M	0.60		NCI/ADR-RES	0.66
	NCI-H460	0.68		SK-OV-3	0.63
	NCI-H522	0.10		786-0	1.0
	COLO 205	0.63	Renal Cancer	A498	0.51
Colon Cancer	HCC-2998	0.59		ACHN	0.55
	HCT-116	0.44		CAKI-1	0.66
	HCT-15	0.69		RXF393	/
	HT29	0.51		SN12C	0.72
	KM12	0.56		TK-10	0.52
	SW-620	0.45		UO-31	/
CNS Cancer	SF-268	0.47	Prostate Cancer	PC-3	0.63
	SF-295	/		DU-145	0.47
	SF-539	0.60		MCF7	0.65
	SNB-19	1.0		MDA-MB-231/ATCC	0.69
	SNB-75	0.35		HS 578T	0.14
	U251	/	Breast Cancer	BT-549	/
Melanoma	LOX IMVI	0.69		T-47D	0.43
				MDA-MB-468	/

of triazolopyridine derivatives were designed through the amalgamation of HDACi pharmacophore and JAK inhibitor Filgotinib to single molecule based on the known binding mode. The fused molecules were confirmed to retain the essential interactions with both proteins in enzymatic assay to exert desired biological functions. In cellular assay, compounds 16a, 16b, 16c, 16j and 19 showed potent antiproliferative activity against human MM cell line RPMI-8226 and breast cancer cell line MDA-MB-231. Further screening of representative 19 demonstrated that these triazolopyridines had broad-spectrum efficacy against solid tumour cell lines such as colon, melanoma, ovarian, and breast cancers as well as hematopoietic cell lines. Overall, the development of JAK and HDAC dual inhibitors maybe a valuable strategy to circumvent resistance. Currently, these triazolopyridines are further studied in our lab.

Experimental section

Chemistry

All reagents and solvents were purchased from Bide Pharmatech Ltd. (Shanghai, China) and Energy Chemical (Shanghai, China). All reactions were monitored using thin layer chromatography (TLC) on silica gel-coated plates (Merck 60 F254), pre-coated silicone plates and UV visualisation. The silica gel (200–300 mesh) was purchased from Qingdao Marine Chemical Ltd. (Qingdao, China). Bruker DRX-400 (^1H -NMR 400MHz, ^{13}C -NMR 101MHz or ^1H -NMR

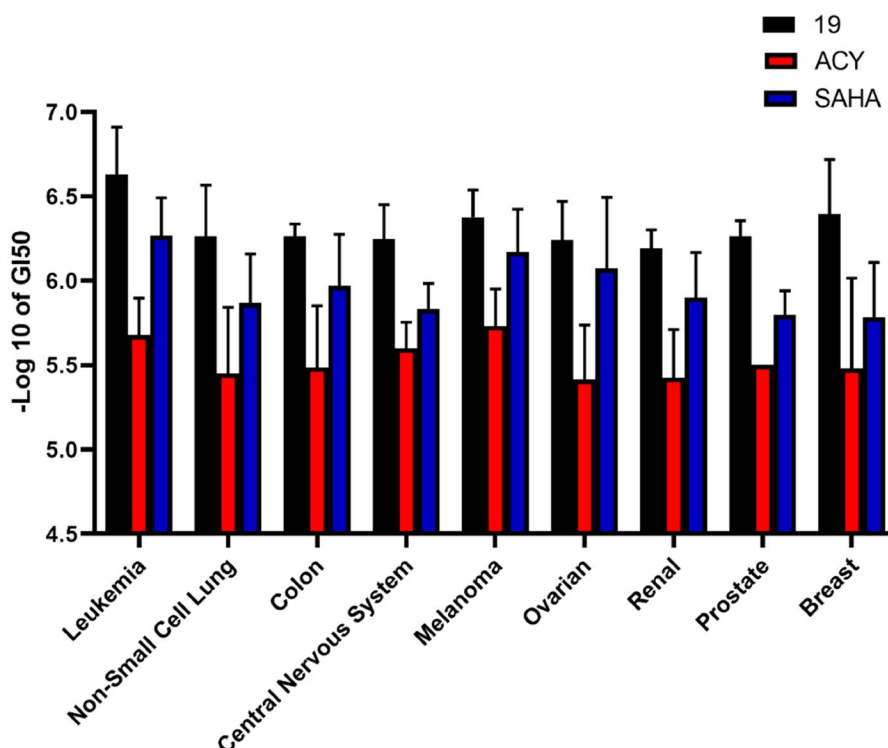


Figure 6. Comparison of the mean GI_{50} values of compound 19 (black), ACY1215 (red), and SAHA (blue) against different tumour cell lines. The y-axis is the $-\log_{10}$ value of GI_{50} .

Table 6. Metabolic stabilities of 19 and SAHA towards HLM.

Compound	HLM Concentration	Substrate Concentration	$T_{1/2}$
19	0.8 mg/mL	0.5 μ M	14.5 h
SAHA	0.8 mg/mL	0.5 μ M	6.8 h

500 MHz, ^{13}C -NMR 126 MHz) were used to detect ^1H and ^{13}C nuclear magnetic resonance (NMR) spectra. The melting points were determined with x-4 instrument (Beijing Tech Instrument Co., Beijing, China) without calibration. All of the target compounds were examined by HPLC on an Agilent Technologies 1260 Infinity equipped with a C18 column (Agilent Zorbax SB-C18, 5 μ M, 4.6 mm \times 150 mm), and the purity of every case was > 95%.

1-(6-Bromo-pyridin-2-yl)-3-carboethoxy-thiourea (12)

To a solution of 2-amino-6-bromopyridine (11) (2.5 g, 14.7 mmol) in dichloromethane (100 ml) cooled to 5 $^{\circ}\text{C}$ was added ethoxycarbonyl isothiocyanate (1.73 ml, 14.7 mmol) dropwise over 15 min. The reaction mixture was then allowed to warm to room temp (20 $^{\circ}\text{C}$) and stirred for 16 h. Evaporation in vacuum gave a solid, which was collected by filtration, thoroughly washed with petrol (3 \times 100 ml), and air-dried to afford 12 which could be used as such for the next step without any purification. Yellow oil, 98.7% yield (crude product). ^1H NMR (400 MHz, Chloroform- d) δ : 12.03 (s, 1H), 8.81 (d, J =7.8 Hz, 1H), 8.15 (s, 1H), 7.60 (t, J =8.0 Hz, 1H), 7.32 (dd, J =7.7, 0.6 Hz, 1H), 4.32–4.30 (m, 2H), 1.35 (t, J =7.1 Hz, 3H).

5-Bromo-[1, 2, 4]triazolo[1, 5-a]pyridin-2-ylamine (13)

To a suspension of hydroxylamine hydrochloride (1.02 g, 14.7 mmol) in EtOH/MeOH (1:1, 100 ml) was added DIPEA (1.45 ml, 8.8 mmol), and the mixture was stirred at r.t. for 1 h. 12 (0.89 g, 2.93 mmol)

was then added and the mixture was refluxed for 3 h. Then, the mixture was allowed to cool and filtered to collect the precipitated solid. The combined solids were washed successively with H_2O (100 ml), EtOH/MeOH (1:1, 100 ml), and Et $_2\text{O}$ (100 ml) and then dried under vacuum to afford the 13 as a white solid, 94.0% yield. ^1H NMR (500 MHz, DMSO- d_6) δ : 7.43–7.33 (m, 2H), 7.24 (dd, J =6.9, 1.7 Hz, 1H), 6.27 (s, 2H).

General procedure for preparation of 14a-m and 17 by Suzuki coupling reaction

To a solution of intermediate 13 in 1, 4-dioxane/water (5: 1), DIPEA (2 equiv) and Pd(dppf) Cl_2 (0.05 equiv) was added corresponding boronic acid (2 equiv). The resulting mixture was then heated at 100 $^{\circ}\text{C}$ for overnight under argon atmosphere. After the reaction was completed, the mixture was allowed to cool and extracted with EtOAc/ H_2O (1: 1) system. The organic layers were dried over anhydrous MgSO_4 and evaporated in vacuum. The product was obtained after purification by flash chromatography.

5-phenyl-[1, 2, 4]triazolo[1, 5-a]pyridin-2-amine (14a). White solid, 45.5% yield. ^1H NMR (500 MHz, DMSO- d_6) δ : 7.97–7.91 (m, 2H), 7.56–7.49 (m, 4H), 7.41–7.35 (m, 1H), 7.01 (d, J =7.2 Hz, 1H), 6.02 (s, 2H).

5-(4-methoxyphenyl)-[1, 2, 4]triazolo[1, 5-a]pyridin-2-amine (14b). White solid, 50.3% yield. ^1H NMR (400 MHz, DMSO- d_6) δ : 7.98–7.91 (m, 2H), 7.51–7.45 (m, 1H), 7.34–7.28 (m, 1H), 7.11–7.05 (m, 2H), 7.00–6.95 (m, 1H), 6.02 (s, 2H), 3.83 (s, 3H).

5-(3-methoxyphenyl)-[1, 2, 4]triazolo[1, 5-a]pyridin-2-amine (14c). White solid, 61.3% yield. ^1H NMR (400 MHz, Chloroform- d) δ : 7.49–7.41 (m, 5H), 7.06–7.01 (m, 1H), 6.92–6.89 (m, 1H), 4.61 (s, 2H), 3.87 (s, 3H).

5-(2-methoxyphenyl)-[1, 2, 4]triazolo[1, 5-a]pyridin-2-amine (14d). White solid, 78.6% yield. ^1H NMR (500 MHz, DMSO- d_6) δ : 7.51–7.42 (m, 2H), 7.40–7.36 (m, 1H), 7.36–7.30 (m, 1H), 7.16 (d, $J=8.4$ Hz, 1H), 7.06 (t, $J=7.4$ Hz, 1H), 6.79 (d, $J=7.1$ Hz, 1H), 5.90 (s, 2H), 3.71 (s, 3H).

5-(p-tolyl)-[1, 2, 4]triazolo[1, 5-a]pyridin-2-amine (14e). White solid, 84.3% yield. ^1H NMR (500 MHz, DMSO- d_6) δ : 7.88–7.84 (m, 2H), 7.51–7.46 (m, 1H), 7.35–7.31 (m, 3H), 7.01–6.97 (m, 1H), 5.99 (s, 2H), 2.39 (s, 3H).

5-(m-tolyl)-[1, 2, 4]triazolo[1, 5-a]pyridin-2-amine (14f). White solid, 51.2% yield. ^1H NMR (400 MHz, DMSO- d_6) δ : 7.75–7.70 (m, 2H), 7.53–7.46 (m, 1H), 7.44–7.38 (m, 1H), 7.37–7.29 (m, 2H), 6.97 (d, $J=7.2$ Hz, 1H), 6.03 (s, 2H), 2.38 (s, 3H).

5-(o-tolyl)-[1, 2, 4]triazolo[1, 5-a]pyridin-2-amine (14g). White solid, 63.4% yield. ^1H NMR (400 MHz, DMSO- d_6) δ : 7.53–7.47 (m, 1H), 7.44–7.29 (m, 5H), 6.82–6.77 (m, 1H), 6.00 (s, 2H), 2.06 (s, 3H).

5-(3-chlorophenyl)-[1, 2, 4]triazolo[1, 5-a]pyridin-2-amine (14h). White solid, 47.6% yield. ^1H NMR (500 MHz, DMSO- d_6) δ : 8.09–8.06 (m, 1H), 7.90–7.87 (m, 1H), 7.59–7.55 (m, 2H), 7.54–7.49 (m, 1H), 7.42–7.37 (m, 1H), 7.10–7.06 (m, 1H), 6.09 (s, 2H).

5-(2-chlorophenyl)-[1, 2, 4]triazolo[1, 5-a]pyridin-2-amine (14i). White solid, 33.5% yield. ^1H NMR (500 MHz, DMSO- d_6) δ : 7.66–7.41 (m, 6H), 6.91–6.85 (m, 1H), 6.04 (s, 2H).

5-(4-fluorophenyl)-[1, 2, 4]triazolo[1, 5-a]pyridin-2-amine (14j). White solid, 59.6% yield. ^1H NMR (500 MHz, DMSO- d_6) δ : 8.04–8.00 (m, 2H), 7.52–7.48 (m, 1H), 7.40–7.34 (m, 3H), 7.04–6.99 (m, 1H), 6.04 (s, 2H).

5-(3, 4-dichlorophenyl)-[1, 2, 4]triazolo[1, 5-a]pyridin-2-amine (14k). White solid, 44.8% yield. ^1H NMR (400 MHz, DMSO- d_6) δ : 8.33–8.30 (m, 1H), 7.97–7.93 (m, 1H), 7.83–7.79 (m, 1H), 7.54–7.49 (m, 1H), 7.43–7.39 (m, 1H), 7.14–7.11 (m, 1H), 6.13 (s, 2H).

5-(4-trifluoromethyl)-[1, 2, 4]triazolo[1, 5-a]pyridin-2-amine (14l). White solid, 57.5% yield. ^1H NMR (500 MHz, DMSO- d_6) δ : 8.17 (d, $J=8.1$ Hz, 2H), 7.91 (d, $J=8.0$ Hz, 2H), 7.54 (t, $J=8.0$ Hz, 1H), 7.43 (d, $J=8.7$ Hz, 1H), 7.11 (d, $J=7.2$ Hz, 1H), 6.09 (s, 2H).

5-(3, 5-bis(trifluoromethyl)phenyl)-[1, 2, 4]triazolo[1, 5-a]pyridin-2-amine (14m). White solid, 45.3% yield. ^1H NMR (400 MHz, DMSO- d_6) δ : 8.66 (s, 2H), 8.27 (s, 1H), 7.58–7.53 (m, 1H), 7.49–7.44 (m, 1H), 7.29–7.24 (m, 1H), 6.14 (s, 2H).

5-(Benzo[d][1, 3]dioxol-5-yl)-[1, 2, 4]triazolo[1, 5-a]pyridin-2-amine (17). White solid, 60.2% yield. ^1H NMR (500 MHz, DMSO- d_6) δ : 7.59–7.58 (m, 1H), 7.49–7.44 (m, 2H), 7.34–7.29 (m, 1H), 7.08–7.05 (m, 1H), 7.00–6.97 (m, 1H), 6.12 (s, 2H), 6.03 (s, 2H).

General procedure for preparation of 15a-m and 18 by reductive amination

To a solution of methyl 4-formylbenzoate (1 equiv) in methanol, appropriate amine (1 equiv), catalytic amount of acetic acid was added. The above solution was stirred at room temperature for

30 min under argon atmosphere. Then, NaBH_3CN (1 equiv) was slowly added in batches and the mixture was stirred for another 6 h. After the reaction was completed, the mixture was diluted with saturated sodium bicarbonate and extracted with ethyl acetate. The combined organic extracts were dried over anhydrous Na_2SO_4 and concentrated under reduced pressure. Purification by flash chromatography (SiO_2 ; ethyl acetate/PE system) yielded the desired compounds.

Methyl 4-(((5-phenyl)-[1, 2, 4]triazolo[1, 5-a]pyridin-2-yl)amino)methyl)benzoate (15a). White solid, 82.4% yield. ^1H NMR (500 MHz, Chloroform- d) δ : 8.02–7.97 (m, 2H), 7.90–7.86 (m, 2H), 7.52–7.42 (m, 6H), 7.38 (d, $J=8.7$ Hz, 1H), 6.90 (d, $J=7.2$ Hz, 1H), 5.00 (s, 1H), 4.68 (d, $J=5.9$ Hz, 2H), 3.90 (s, 3H).

Methyl 4-(((5-(4-methoxyphenyl)-[1, 2, 4]triazolo[1, 5-a]pyridin-2-yl)amino)methyl)benzoate (15b). White solid, 87.5% yield. ^1H NMR (400 MHz, Chloroform- d) δ : 8.02–7.97 (m, 2H), 7.89–7.84 (m, 2H), 7.49–7.39 (m, 3H), 7.36–7.31 (m, 1H), 7.03–6.98 (m, 2H), 6.89–6.84 (m, 1H), 5.06–4.97 (m, 1H), 4.68 (d, $J=6.1$ Hz, 2H), 3.90 (s, 3H), 3.88 (s, 3H).

Methyl 4-(((5-(3-methoxyphenyl)-[1,2,4]triazolo[1,5-a]pyridin-2-yl)amino)methyl)benzoate (15c). White solid, 76.6% yield. ^1H NMR (400 MHz, Chloroform- d) δ : 8.02–7.97 (m, 2H), 7.51–7.37 (m, 7H), 7.04–7.00 (m, 1H), 6.94–6.89 (m, 1H), 5.02 (s, 1H), 4.68 (d, $J=6.1$ Hz, 2H), 3.90 (s, 3H), 3.80 (s, 3H).

Methyl 4-(((5-(2-methoxyphenyl)-[1, 2, 4]triazolo[1, 5-a]pyridin-2-yl)amino)methyl)benzoate (15d). White solid, 77.3% yield. ^1H NMR (400 MHz, Chloroform- d) δ : 7.95 (d, $J=8.0$ Hz, 2H), 7.48–7.31 (m, 6H), 7.08–6.98 (m, 2H), 6.84–6.79 (m, 1H), 5.31–5.23 (m, 1H), 4.60 (d, $J=6.2$ Hz, 2H), 3.88 (s, 3H).

Methyl 4-(((5-(p-tolyl)-[1, 2, 4]triazolo[1, 5-a]pyridin-2-yl)amino)methyl)benzoate (15e). White solid, 75.2% yield. ^1H NMR (500 MHz, Chloroform- d) δ : 7.98 (d, $J=8.1$ Hz, 2H), 7.78 (d, $J=7.9$ Hz, 2H), 7.45 (d, $J=8.1$ Hz, 2H), 7.42–7.37 (m, 1H), 7.33–7.25 (m, 3H), 6.88–6.83 (m, 1H), 5.34–5.27 (m, 1H), 4.64 (d, $J=6.2$ Hz, 2H), 3.89 (s, 3H), 2.41 (s, 3H).

Methyl 4-(((5-(m-tolyl)-[1, 2, 4]triazolo[1, 5-a]pyridin-2-yl)amino)methyl)benzoate (15f). White solid, 71.4% yield. ^1H NMR (400 MHz, Chloroform- d) δ : 8.01–7.96 (m, 2H), 7.69–7.64 (m, 2H), 7.48–7.33 (m, 5H), 7.28 (d, $J=7.7$ Hz, 1H), 6.89–6.85 (m, 1H), 5.14 (t, $J=6.3$ Hz, 1H), 4.66 (d, $J=6.2$ Hz, 2H), 3.90 (s, 3H), 2.41 (s, 3H).

Methyl 4-(((5-(o-tolyl)-[1, 2, 4]triazolo[1, 5-a]pyridin-2-yl)amino)methyl)benzoate (15g). White solid, 76.5% yield. ^1H NMR (400 MHz, Chloroform- d) δ : 7.87 (d, $J=8.0$ Hz, 2H), 7.35–7.27 (m, 5H), 7.26–7.18 (m, 3H), 6.66–6.61 (m, 1H), 5.31 (t, $J=6.3$ Hz, 1H), 4.51 (d, $J=6.3$ Hz, 2H), 3.81 (s, 3H), 2.00 (s, 3H).

Methyl 4-(((5-(3-chlorophenyl)-[1, 2, 4]triazolo[1, 5-a]pyridin-2-yl)amino)methyl)benzoate (15h). White solid, 78.3% yield. ^1H NMR (500 MHz, Chloroform- d) δ : 8.00 (d, $J=8.1$ Hz, 2H), 7.96–7.93 (m, 1H), 7.78–7.74 (m, 1H), 7.49–7.38 (m, 6H), 6.92–6.89 (m, 1H), 5.08–5.02 (m, 1H), 4.67 (d, $J=5.9$ Hz, 2H), 3.90 (s, 3H).

Methyl 4-(((5-(2-chlorophenyl)-[1, 2, 4]triazolo[1, 5-a]pyridin-2-yl)amino)methyl)benzoate (15i). White solid, 82.0% yield. ^1H NMR

(500MHz, Chloroform-*d*) δ : 8.00–7.94 (*m*, 2H), 7.57–7.52 (*m*, 1H), 7.51–7.38 (*m*, 7H), 6.86–6.79 (*m*, 1H), 5.03–4.96 (*m*, 1H), 4.67–4.60 (*m*, 2H), 3.90 (*s*, 3H).

Methyl 4-(((5-(4-fluorophenyl)-[1, 2, 4]triazolo[1, 5-*a*]pyridin-2-yl)amino)methyl)benzoate (15j). White solid, 81.4% yield. ^1H NMR (500MHz, Chloroform-*d*) δ : 8.01–7.97 (*m*, 2H), 7.91–7.86 (*m*, 2H), 7.47–7.40 (*m*, 3H), 7.37–7.34 (*m*, 1H), 7.17 (*t*, $J=8.6\text{ Hz}$, 2H), 6.88–6.84 (*m*, 1H), 5.16 (*t*, $J=6.4\text{ Hz}$, 1H), 4.66 (*d*, $J=6.1\text{ Hz}$, 2H), 3.90 (*s*, 3H).

Methyl 4-(((5-(3, 4-dichlorophenyl)-[1,2,4]triazolo[1, 5-*a*]pyridin-2-yl)amino)methyl)benzoate (15k). White solid, 69.7% yield. ^1H NMR (500MHz, Chloroform-*d*) δ : 8.08–8.06 (*m*, 1H), 8.02–7.99 (*m*, 2H), 7.75–7.71 (*m*, 1H), 7.57–7.53 (*m*, 1H), 7.48–7.38 (*m*, 4H), 6.91–6.88 (*m*, 1H), 5.15–5.10 (*m*, 1H), 4.66 (*d*, $J=6.3\text{ Hz}$, 2H), 3.90 (*s*, 3H).

Methyl 4-(((5-(4-(trifluoromethyl)phenyl)-[1, 2, 4]triazolo[1, 5-*a*]pyridin-2-yl)amino)methyl)benzoate (15l). White solid, 77.3% yield. ^1H NMR (500MHz, Chloroform-*d*) δ : 8.03–7.99 (*m*, 4H), 7.75 (*d*, $J=8.1\text{ Hz}$, 2H), 7.49–7.42 (*m*, 4H), 6.95–6.91 (*m*, 1H), 5.09–5.02 (*m*, 1H), 4.67 (*d*, $J=6.0\text{ Hz}$, 2H), 3.91 (*d*, $J=1.1\text{ Hz}$, 3H).

Methyl 4-(((5-(3, 5-bis(trifluoromethyl)phenyl)-[1, 2, 4]triazolo[1, 5-*a*]pyridin-2-yl)amino)methyl)benzoate (15m). White solid, 74.5% yield. ^1H NMR (400MHz, Chloroform-*d*) δ : 8.45 (*s*, 2H), 8.01–7.96 (*m*, 3H), 7.52–7.43 (*m*, 4H), 7.02–6.98 (*m*, 1H), 5.22–5.16 (*m*, 1H), 4.65 (*d*, $J=6.3\text{ Hz}$, 2H), 3.90 (*s*, 3H).

Methyl 4-(((5-(benzo[d][1, 3]dioxol-5-yl)-[1, 2, 4]triazolo[1, 5-*a*]pyridin-2-yl)amino)methyl)benzoate (18). White solid, 79.2% yield. ^1H NMR (500MHz, Chloroform-*d*) δ : 8.04–7.98 (*m*, 2H), 7.51–7.30 (*m*, 6H), 6.95–6.83 (*m*, 2H), 6.06 (*s*, 2H), 5.08–5.00 (*m*, 1H), 4.68 (*d*, $J=6.5\text{ Hz}$, 2H), 3.91 (*s*, 3H).

5.1.5. The detailed procedure for preparation of target compounds 16a-m and 19 by aminolysis reaction could be found in Ref. 9

N-hydroxy-4-(((5-phenyl-[1, 2, 4]triazolo[1, 5-*a*]pyridin-2-yl)amino)methyl)benzamide (16a). White solid, 58.4% yield. m.p.: 1 5 1 ~ 153 °C. ^1H NMR (500MHz, DMSO-*d*₆) δ : 11.14 (*s*, 1H), 8.96 (*s*, 1H), 7.96–7.89 (*m*, 2H), 7.69 (*d*, $J=8.1\text{ Hz}$, 2H), 7.55–7.49 (*m*, 4H), 7.40 (*t*, $J=8.3\text{ Hz}$, 3H), 7.34–7.29 (*m*, 1H), 7.05 (*d*, $J=7.3\text{ Hz}$, 1H), 4.46 (*d*, $J=5.1\text{ Hz}$, 2H). ^{13}C NMR (126MHz, DMSO) δ : 165.67, 164.18, 151.30, 144.04, 138.59, 132.45, 131.10, 129.56, 129.20, 128.83, 128.24, 127.10, 126.72, 111.64, 111.45, 45.69. HR-MS (ESI) calcd. $\text{C}_{20}\text{H}_{17}\text{N}_5\text{O}_2$, $[\text{M}+\text{H}]^+$ *m/z*: 360.14550, found: 360.14505.

N-hydroxy-4-(((5-(4-methoxyphenyl)-[1, 2, 4]triazolo[1, 5-*a*]pyridin-2-yl)amino)methyl)benzamide (16b). White solid, 65.0% yield. m.p.: 1 4 0 ~ 141 °C. ^1H NMR (400MHz, DMSO-*d*₆) δ : 11.15 (*s*, 1H), 8.99 (*s*, 1H), 7.96–7.90 (*m*, 2H), 7.72–7.67 (*m*, 2H), 7.52–7.46 (*m*, 1H), 7.42 (*d*, $J=8.0\text{ Hz}$, 2H), 7.36–7.32 (*m*, 1H), 7.32–7.27 (*m*, 1H), 7.10–7.05 (*m*, 2H), 7.04–6.99 (*m*, 1H), 4.47 (*d*, $J=5.8\text{ Hz}$, 2H), 3.84 (*s*, 3H). ^{13}C NMR (126MHz, DMSO-*d*₆) δ : 165.64, 164.23, 160.22, 151.43, 144.17, 138.51, 131.11, 130.40, 129.28, 127.16, 126.79, 124.68, 113.68, 110.97, 110.73, 55.38, 45.74. HR-MS (ESI) calcd. $\text{C}_{21}\text{H}_{19}\text{N}_5\text{O}_3$, $[\text{M}+\text{H}]^+$ *m/z*: 390.15607, found: 390.15605.

N-hydroxy-4-(((5-(3-methoxyphenyl)-[1, 2, 4]triazolo[1, 5-*a*]pyridin-2-yl)amino)methyl)benzamide (16c). White solid, 68.7% yield. m.p.:

1 2 9 ~ 131 °C. ^1H NMR (400MHz, DMSO-*d*₆) δ : 11.14 (*s*, 1H), 8.98 (*s*, 1H), 7.71–7.66 (*m*, 2H), 7.58–7.55 (*m*, 1H), 7.54–7.43 (*m*, 3H), 7.43–7.38 (*m*, 3H), 7.34–7.29 (*m*, 1H), 7.11–7.05 (*m*, 2H), 4.47 (*d*, $J=6.3\text{ Hz}$, 2H), 3.77 (*s*, 3H). ^{13}C NMR (126MHz, DMSO-*d*₆) δ : 165.75, 164.23, 158.94, 151.43, 144.09, 138.42, 133.69, 131.12, 129.44, 129.24, 127.04, 126.81, 121.14, 115.29, 114.46, 111.78, 111.58, 55.22, 45.66. HR-MS (ESI) calcd. $\text{C}_{21}\text{H}_{19}\text{N}_5\text{O}_3$, $[\text{M}+\text{H}]^+$ *m/z*: 390.15607, found: 390.15604.

N-hydroxy-4-(((5-(2-methoxyphenyl)-[1, 2, 4]triazolo[1, 5-*a*]pyridin-2-yl)amino)methyl)benzamide (16d). White solid, 70.8% yield. m.p.: 1 4 0 ~ 141 °C. ^1H NMR (500MHz, DMSO-*d*₆) δ : 11.13 (*s*, 1H), 8.97 (*s*, 1H), 7.69–7.63 (*m*, 2H), 7.52–7.45 (*m*, 2H), 7.40–7.34 (*m*, 4H), 7.21–7.15 (*m*, 2H), 7.09–7.05 (*m*, 1H), 6.85–6.82 (*m*, 1H), 4.42 (*d*, $J=6.4\text{ Hz}$, 2H), 3.66 (*s*, 3H). ^{13}C NMR (126MHz, DMSO-*d*₆) δ : 165.74, 164.21, 157.05, 150.74, 144.20, 136.87, 131.09, 131.04, 130.65, 128.60, 126.99, 126.76, 122.13, 120.27, 112.79, 111.72, 111.37, 55.53, 45.57. HR-MS (ESI) calcd. $\text{C}_{21}\text{H}_{19}\text{N}_5\text{O}_3$, $[\text{M}+\text{H}]^+$ *m/z*: 390.15607, found: 390.15594.

N-hydroxy-4-(((5-(*p*-tolyl)-[1, 2, 4]triazolo[1, 5-*a*]pyridin-2-yl)amino)methyl)benzamide (16e). White solid, 73.0% yield. m.p.: 1 3 5 ~ 136 °C. ^1H NMR (500MHz, DMSO-*d*₆) δ : 11.13 (*s*, 1H), 8.96 (*s*, 1H), 7.84 (*d*, $J=8.2\text{ Hz}$, 2H), 7.69 (*d*, $J=8.1\text{ Hz}$, 2H), 7.53–7.48 (*m*, 1H), 7.42 (*d*, $J=7.9\text{ Hz}$, 2H), 7.38–7.32 (*m*, 3H), 7.30–7.25 (*m*, 1H), 7.04–7.01 (*m*, 1H), 4.46 (*d*, $J=6.1\text{ Hz}$, 2H), 2.40 (*s*, 3H). ^{13}C NMR (126MHz, DMSO-*d*₆) δ : 165.65, 164.20, 151.37, 144.09, 139.32, 138.68, 131.10, 129.59, 129.20, 128.80, 128.72, 127.12, 126.73, 111.28, 111.12, 45.69, 20.96. HR-MS (ESI) calcd. $\text{C}_{21}\text{H}_{19}\text{N}_5\text{O}_2$, $[\text{M}+\text{H}]^+$ *m/z*: 374.16115, found: 374.16119.

N-hydroxy-4-(((5-(*m*-tolyl)-[1, 2, 4]triazolo[1, 5-*a*]pyridin-2-yl)amino)methyl)benzamide (16f). White solid, 69.3% yield. m.p.: 1 2 1 ~ 122 °C. ^1H NMR (500MHz, DMSO-*d*₆) δ : 11.14 (*s*, 1H), 8.97 (*s*, 1H), 7.75–7.67 (*m*, 4H), 7.53–7.48 (*m*, 1H), 7.44–7.36 (*m*, 4H), 7.33–7.28 (*m*, 2H), 7.03–7.00 (*m*, 1H), 4.46 (*d*, $J=6.4\text{ Hz}$, 2H), 2.38 (*s*, 3H). ^{13}C NMR (126MHz, DMSO-*d*₆) δ : 165.68, 164.18, 151.34, 144.08, 138.76, 137.43, 132.44, 131.09, 130.17, 129.26, 129.15, 128.13, 127.06, 126.75, 125.99, 111.58, 111.34, 45.67, 21.03. HR-MS (ESI) calcd. $\text{C}_{21}\text{H}_{19}\text{N}_5\text{O}_2$, $[\text{M}+\text{H}]^+$ *m/z*: 374.16115, found: 374.16113.

N-hydroxy-4-(((5-(*o*-tolyl)-[1, 2, 4]triazolo[1, 5-*a*]pyridin-2-yl)amino)methyl)benzamide (16g). White solid, 74.6% yield. m.p.: 1 2 8 ~ 129 °C. ^1H NMR (500MHz, DMSO-*d*₆) δ : 11.13 (*s*, 1H), 8.96 (*s*, 1H), 7.66 (*d*, $J=8.0\text{ Hz}$, 2H), 7.54–7.48 (*m*, 1H), 7.45–7.39 (*m*, 2H), 7.37–7.29 (*m*, 5H), 7.25 (*t*, $J=6.4\text{ Hz}$, 1H), 6.84–6.80 (*m*, 1H), 4.41 (*d*, $J=6.3\text{ Hz}$, 2H), 2.00 (*s*, 3H). ^{13}C NMR (126MHz, DMSO-*d*₆) δ : 166.02, 164.18, 150.76, 144.00, 139.27, 136.94, 133.07, 131.07, 129.90, 129.55, 129.39, 128.87, 126.99, 126.73, 125.74, 112.34, 111.47, 45.57, 19.20. HR-MS (ESI) calcd. $\text{C}_{21}\text{H}_{19}\text{N}_5\text{O}_2$, $[\text{M}+\text{H}]^+$ *m/z*: 374.16115, found: 374.16116.

4-(((5-(3-chlorophenyl)-[1, 2, 4]triazolo[1, 5-*a*]pyridin-2-yl)amino)methyl)-N-hydroxybenzamide (16h). White solid, 63.5% yield. m.p.: 1 1 8 ~ 120 °C. ^1H NMR (500MHz, DMSO-*d*₆) δ : 11.13 (*s*, 1H), 8.97 (*s*, 1H), 8.12–8.09 (*m*, 1H), 7.89–7.86 (*m*, 1H), 7.69 (*d*, $J=8.1\text{ Hz}$, 2H), 7.60–7.51 (*m*, 3H), 7.45–7.37 (*m*, 4H), 7.15–7.11 (*m*, 1H), 4.46 (*d*, $J=6.2\text{ Hz}$, 2H). ^{13}C NMR (126MHz, DMSO-*d*₆) δ : 165.70, 164.20, 151.32, 144.00, 136.91, 134.32, 132.94, 131.13, 130.22, 129.47, 129.20, 128.56, 127.53, 127.15, 126.79, 112.11, 112.05, 45.68. HR-MS (ESI) calcd. $\text{C}_{20}\text{H}_{16}\text{ClN}_5\text{O}_2$, $[\text{M}+\text{H}]^+$ *m/z*: 394.10653, found:

394.10654. $C_{20}H_{16}Cl^{37}N_5O_2$, $[M+H]^+$ m/z : 396.10358, found: 396.10312.

4-(((5-(2-chlorophenyl)-[1, 2, 4]triazolo[1, 5-a]pyridin-2-yl)amino)methyl)-N-hydroxybenzamide (16i). White solid, 57.2% yield. m.p.: 121–123°C. 1H NMR (500 MHz, DMSO- d_6) δ : 11.12 (s, 1H), 8.96 (s, 1H), 7.67–7.62 (m, 3H), 7.58–7.50 (m, 4H), 7.49–7.45 (m, 1H), 7.36 (d, $J=8.1$ Hz, 2H), 7.29 (t, $J=6.4$ Hz, 1H), 6.93–6.90 (m, 1H), 4.43 (d, $J=6.4$ Hz, 2H). ^{13}C NMR (101 MHz, DMSO- d_6) δ : 166.03, 150.65, 144.03, 136.42, 132.94, 132.28, 131.65, 131.28, 131.12, 129.52, 128.76, 127.39, 127.10, 126.78, 112.80, 112.27, 45.57. HR-MS (ESI) calcd. $C_{20}H_{16}Cl^{35}N_5O_2$, $[M+H]^+$ m/z : 394.10653, found: 394.10651. $C_{20}H_{16}Cl^{37}N_5O_2$, $[M+H]^+$ m/z : 396.10358, found: 396.10291.

4-(((5-(4-fluorophenyl)-[1, 2, 4]triazolo[1, 5-a]pyridin-2-yl)amino)methyl)-N-hydroxybenzamide (16j). White solid, 63.8% yield. m.p.: 114–115°C. 1H NMR (500 MHz, DMSO- d_6) δ : 11.16 (s, 1H), 8.97 (s, 1H), 8.03–7.98 (m, 2H), 7.72–7.68 (m, 2H), 7.54–7.49 (m, 1H), 7.44–7.31 (m, 6H), 7.08–7.04 (m, 1H), 4.46 (d, $J=6.3$ Hz, 2H). ^{13}C NMR (126 MHz, DMSO- d_6) δ : 165.67, 161.62, 151.31, 144.03, 137.54, 131.28, 131.22, 131.08, 129.20, 128.85, 127.10, 126.76, 115.22, 111.55, 45.69. HR-MS (ESI) calcd. $C_{20}H_{16}FN_5O_2$, $[M+H]^+$ m/z : 378.13608, found: 378.13602.

4-(((5-(3, 4-dichlorophenyl)-[1, 2, 4]triazolo[1, 5-a]pyridin-2-yl)amino)methyl)-N-hydroxybenzamide (16k). White solid, 51.3% yield. m.p.: 126–127°C. 1H NMR (400 MHz, DMSO- d_6) δ : 11.14 (s, 1H), 8.98 (s, 1H), 8.34–8.31 (m, 1H), 7.95–7.92 (m, 1H), 7.83–7.79 (m, 1H), 7.72–7.67 (m, 2H), 7.61–7.51 (m, 2H), 7.46–7.38 (m, 4H), 7.19–7.16 (m, 1H), 4.46 (d, $J=6.4$ Hz, 2H). ^{13}C NMR (126 MHz, DMSO- d_6) δ : 165.68, 164.16, 151.30, 148.07, 143.94, 135.85, 132.71, 132.20, 130.65, 130.45, 129.01, 128.68, 127.10, 126.78, 126.37, 112.33, 112.11, 45.67. HR-MS (ESI) calcd. $C_{20}H_{15}Cl^{35}_2N_5O_2$, $[M+H]^+$ m/z : 428.06756, found: 428.06757. $C_{20}H_{15}Cl^{35}Cl^{37}N_5O_2$, $[M+H]^+$ m/z : 430.06461, found: 428.06442. $C_{20}H_{15}Cl^{37}_2N_5O_2$, $[M+H]^+$ m/z : 432.06116, found: 432.06082.

N-hydroxy-4-(((5-(4-(trifluoromethyl)phenyl)-[1, 2, 4]triazolo[1, 5-a]pyridin-2-yl)amino)methyl)benzamide (16l). White solid, 55.2% yield. m.p.: 132–134°C. 1H NMR (400 MHz, DMSO- d_6) δ : 11.15 (s, 1H), 8.98 (s, 1H), 8.16 (d, $J=8.1$ Hz, 2H), 7.90 (d, $J=8.3$ Hz, 2H), 7.71–7.67 (m, 2H), 7.58–7.53 (m, 1H), 7.48–7.35 (m, 4H), 7.17–7.13 (m, 1H), 4.47 (d, $J=6.4$ Hz, 2H). ^{13}C NMR (126 MHz, DMSO- d_6) δ : 165.77, 164.18, 151.28, 143.96, 136.94, 136.34, 131.14, 129.79, 129.71, 129.21, 127.10, 126.75, 125.17, 125.14, 125.11, 125.08, 112.42, 112.32. HR-MS (ESI) calcd. $C_{21}H_{16}F_3N_5O_2$, $[M+H]^+$ m/z : 428.13289, found: 428.13284.

4-(((5-(3, 5-bis(trifluoromethyl)phenyl)-[1, 2, 4]triazolo[1, 5-a]pyridin-2-yl)amino)methyl)-N-hydroxybenzamide (16m). White solid, 44.5% yield. m.p.: 138–139°C. 1H NMR (500 MHz, DMSO- d_6) δ : 11.15 (s, 1H), 9.00 (s, 1H), 8.70 (s, 2H), 8.28 (s, 1H), 7.69–7.65 (m, 2H), 7.60–7.56 (m, 1H), 7.53–7.49 (m, 1H), 7.47–7.43 (m, 1H), 7.42–7.38 (m, 2H), 7.37–7.33 (m, 1H), 4.45 (d, $J=6.4$ Hz, 2H). ^{13}C NMR (101 MHz, DMSO- d_6) δ : 166.03, 150.65, 144.03, 136.42, 132.94, 132.28, 131.65, 131.28, 131.12, 129.52, 128.76, 127.39, 127.10, 126.78, 112.80, 112.27, 45.57. HR-MS (ESI) calcd. $C_{22}H_{15}F_6N_5O_2$, $[M+H]^+$ m/z : 496.12027, found: 496.12021.

4-(((5-(Benzo[d][1, 3]dioxol-5-yl)-[1, 2, 4]triazolo[1, 5-a]pyridin-2-yl)amino)methyl)-N-hydroxybenzamide (19). White solid, 67.8% yield. m.p.: 136–137°C. 1H NMR (400 MHz, DMSO- d_6) δ : 11.14 (s, 1H),

8.97 (s, 1H), 7.71–7.67 (m, 2H), 7.58–7.57 (m, 1H), 7.49–7.45 (m, 2H), 7.44–7.40 (m, 2H), 7.36–7.31 (m, 2H), 7.08–7.05 (m, 1H), 7.04–7.01 (m, 1H), 6.13 (s, 2H), 4.46 (d, $J=6.4$ Hz, 2H). ^{13}C NMR (126 MHz, DMSO- d_6) δ : 165.63, 151.39, 148.30, 147.06, 144.09, 138.27, 131.12, 129.17, 128.02, 127.13, 126.77, 126.10, 123.34, 111.25, 110.98, 109.19, 108.14, 101.56, 45.69. HR-MS (ESI) calcd. $C_{21}H_{17}N_5O_4$, $[M+H]^+$ m/z : 404.13533, found: 404.13528.

In vitro HDAC enzyme assay

IC₅₀ testing of compounds was performed by Reaction Biology Corporation using fluorescent activity assay. The detailed protocol can be found in Ref. 9 or on the website (<https://www.reactionbiology.com/services/target-specific-assays/epigenetic-assays/hdac-assays/>). The assay for HDAC10 activity was performed at German Cancer Research Centre (69210 Heidelberg, Germany). The detailed protocol could be found in Ref. 9.

Kinase inhibition assay

IC₅₀ testing of compounds was performed by Reaction Biology Corporation. In brief, evaluation of the effects of compounds on the activity of the human JAKs was quantified by measuring the phosphorylation of the substrate Ulight-CAGAGAIETDKEYTVKD using human recombinant enzymes and the LANCE detection method. Other kinase inhibition assays were performed as the above method. Origin data analysis software was used to calculate the IC₅₀ data by the nonlinear curve fitting method.

Cell culture and cell viability assay

MDA-MB-231 cells (purchased from the Chinese Academy of Sciences Cell Bank) were cultured in DMEM with 10% foetal bovine serum (FBS) and RPMI-8226 (purchased from Wuhan Pricella Biotechnology Co., Ltd.) were cultured in IMDM medium with 20% FBS, 100 U/mL penicillin and 100 µg/mL streptomycin. All cells were kept in humidified air at 37°C with 5% CO₂. The measurement of cell growth inhibition was conducted as described previously⁹.

For NCI-60 screening, all detailed test method is described on the NCI Web site (https://dtp.cancer.gov/discovery_development/nci-60/methodology.htm).

Apoptosis assay

For flow cytometry assay, annexin V-FITC/propidium iodide (PI) staining assay (A211-02, Vazyme) was employed to detect cells in early apoptotic and late apoptotic stages. Cells were seeded in 6-well plates and incubated overnight, then treated with DMSO or compounds for 48 h, harvested and washed in cold PBS. After incubation with 100 µL of annexin V-FITC/PI staining solution, the cells were collected and analysed by FACS Calibur (BD, USA), and data were analysed using FlowJo 7.6 Software.

Computational methods

Sybyl-X 2.0 software (2225 Central Ave Ste 1008, Saint Louis, MO 63105, USA) was used for molecular docking. The cocrystal of HDAC6 (PDB: 5EDU) and JAK2 (PDB: 4P7E) were used as the receptors, respectively. The cavity occupied by TSA or Filgotinib was selected as the binding site. The detailed protocol could be found in Ref. 10.

Microsomal stability assay

Human liver microsome was purchased from Research Institute for Liver Disease (Shanghai) Co., Ltd. NADPH was purchased from Roche. Each incubated mixture contained 0.8 mg/mL human liver microsome, 50 μ L magnesium chloride, 60 μ L potassium phosphate buffer (pH 7.4) and 0.5 μ M tested compound in a total volume of 200 μ L. After prewarming at 37°C for 5 min, 50 μ L NADPH was added to initiate the reaction. The reaction was terminated after 0, 5, 10, 15, 30, 60 or 90 min by adding 400 μ L ice-cold ethyl acetate into 200 μ L of incubation mixture. The sample was then centrifuged at 4000 rpm for 10 min at 4°C. The supernatant was then analysed by LC-MS/MS.

Acknowledgement

We thank Jing Shi and Dr. Xin Chen for compound design and synthesis based on their previous work (DOI: 10.1016/j.ejmech.2023.115776 and 10.1039/D4RA01672F).

Author contributions

Conceptualisation: Zhengshui Xu, Xin Chen and Shiyuan Liu; Methodology: Zhengshui Xu and Changchun Ye; Validation: Xingjie Wang, Ranran Kong and Zilu Chen; Formal analysis: Zhengshui Xu and Jing Shi; Writing—original draft preparation: Zhengshui Xu and Xin Chen. Writing—review and editing: Xin Chen and Shiyuan Liu. All authors have read and agreed to the published version of the manuscript.

Declaration of competing interest

The authors declare that they have no known competing financial interests or personal relationships that could have appeared to influence the work reported in this paper.

Funding

This work was funded by the [National Natural Science Foundation of China] under Grant [number 82303811 and 82373002], the [Natural Science Basic Research Program of Shaanxi Province] under Grant [number 2023-JC-QN-0840] and the [Key Research and Development Program of Shaanxi Province] under Grant [number 2023-YBSF-359].

ORCID

Xin Chen  <http://orcid.org/0000-0001-8623-7655>

Data availability statement

The datasets presented in the current study are available from the corresponding author upon reasonable request.

References

- Shirvaliloo M. The landscape of histone modifications in epigenomics since 2020. *Epigenomics*. 2022;14(23):1465–1477.
- Zhang Y, Sun Z, Jia J, Du T, Zhang N, Tang Y, Fang Y, Fang D. Overview of histone modification. *Adv Exp Med Biol*. 2021;1283:1–16.
- Gediya P, Parikh PK, Vyas VK, Ghate MD. Histone deacetylase 2: A potential therapeutic target for cancer and neurodegenerative disorders. *Eur J Med Chem*. 2021;216:113332.
- Cheng B, Pan W, Xiao Y, Ding Z, Zhou Y, Fei X, Liu J, Su Z, Peng X, Chen J, et al. HDAC-targeting epigenetic modulators for cancer immunotherapy. *Eur J Med Chem*. 2024;265:116129.
- de Ruijter AJM, van Gennip AH, Caron HN, Kemp S, van Kuilenburg ABP. Histone deacetylases (HDACs): characterization of the classical HDAC family. *Biochem J*. 2003;370(Pt 3):737–749.
- Gregoret IV, Lee YM, Goodson HV. Molecular evolution of the histone deacetylase family: functional implications of phylogenetic analysis. *J Mol Biol*. 2004;338(1):17–31.
- Ho TCS, Chan AHY, Ganesan A. Thirty Years of HDAC Inhibitors: 2020 Insight and Hindsight. *J Med Chem*. 2020;63(21):12460–12484.
- Zhang W-X, Huang J, Tian X-Y, Liu Y-H, Jia M-Q, Wang W, Jin C-Y, Song J, Zhang S-Y. A review of progress in o-aminobenzamide-based HDAC inhibitors with dual targeting capabilities for cancer therapy. *Eur J Med Chem*. 2023;259:115673.
- Chen X, Wang J, Zhao P, Dang B, Liang T, Steimbach RR, Miller AK, Liu J, Wang X, Zhang T, et al. Tetrahydro-beta-carboline derivatives as potent histone deacetylase 6 inhibitors with broad-spectrum antiproliferative activity. *Eur J Med Chem*. 2023;260:115776.
- Chen X, Chen X, Steimbach RR, Wu T, Li H, Dan W, Shi P, Cao C, Li D, Miller AK, et al. Novel 2, 5-diketopiperazine derivatives as potent selective histone deacetylase 6 inhibitors: Rational design, synthesis and antiproliferative activity. *Eur J Med Chem*. 2020;187:111950.
- Chen X, Zhao S, Li H, Wang X, Geng A, Cui H, Lu T, Chen Y, Zhu Y. Design, synthesis and biological evaluation of novel isoindolinone derivatives as potent histone deacetylase inhibitors. *Eur J Med Chem*. 2019;168:110–122.
- Gao Y, Duan J, Dang X, Yuan Y, Wang Y, He X, Bai R, Ye X-Y, Xie T. Design, synthesis and biological evaluation of novel histone deacetylase (HDAC) inhibitors derived from beta-elemene scaffold. *J Enzyme Inhib Med Chem*. 2023;38(1):2195991.
- Mehndiratta S, Chen M-C, Chao Y-H, Lee C-H, Liou J-P, Lai M-J, Lee H-Y. Effect of 3-substitution of quinolinehydroxamic acids on selectivity of histone deacetylase isoforms. *J Enzyme Inhib Med Chem*. 2021;36(1):74–84.
- Pun MD, Wu H-H, Olatunji FP, Kesic BN, Peters JW, Berkman CE. Phosphorus containing analogues of SAHA as inhibitors of HDACs. *J Enzyme Inhib Med Chem*. 2022;37(1):1315–1319.
- Marks PA, Breslow R. Dimethyl sulfoxide to vorinostat: development of this histone deacetylase inhibitor as an anticancer drug. *Nat Biotechnol*. 2007;25(1):84–90.
- Sawas A, Radeski D, O'Connor OA. Belinostat in patients with refractory or relapsed peripheral T-cell lymphoma: a perspective review. *Ther Adv Hematol*. 2015;6(4):202–208.
- Laubach JP, Moreau P, San-Miguel JF, Richardson PG. Panobinostat for the treatment of multiple myeloma. *Clin Cancer Res*. 2015;21(21):4767–4773.
- Reddy SA. Romidepsin for the treatment of relapsed/refractory cutaneous T-cell lymphoma (mycosis fungoides/Sezary syndrome): Use in a community setting. *Crit Rev Oncol Hematol*. 2016;106:99–107.

19. Dong M, Ning Z-Q, Xing P-Y, Xu J-L, Cao H-X, Dou G-F, Meng Z-Y, Shi Y-K, Lu X-P, Feng F-Y, et al. Phase I study of chidamide (CS055/HBI-8000), a new histone deacetylase inhibitor, in patients with advanced solid tumors and lymphomas. *Cancer Chemother Pharmacol.* 2012;69(6):1413–1422.
20. Liang T, Wang F, Elhassan RM, Cheng Y, Tang X, Chen W, Fang H, Hou X. Targeting histone deacetylases for cancer therapy: trends and challenges. *Acta Pharm Sin B.* 2023;13(6):2425–2463.
21. Shirbhate E, Singh V, Jahoriya V, Mishra A, Veerasamy R, Tiwari AK, Rajak H. Dual inhibitors of HDAC and other epigenetic regulators: a novel strategy for cancer treatment. *Eur J Med Chem.* 2024;263:115938.
22. Bass AKA, El-Zoghbi MS, Nageeb E-SM, Mohamed MFA, Badr M, Abuo-Rahma GE-DA. Comprehensive review for anticancer hybridized multitargeting HDAC inhibitors. *Eur J Med Chem.* 2021;209:112904.
23. Peng X, Sun Z, Kuang P, Chen J. Recent progress on HDAC inhibitors with dual targeting capabilities for cancer treatment. *Eur J Med Chem.* 2020;208:112831.
24. Wang K-L, Yeh T-Y, Hsu P-C, Wong T-H, Liu J-R, Chern J-W, Lin M-H, Yu C-W. Discovery of novel anaplastic lymphoma kinase (ALK) and histone deacetylase (HDAC) dual inhibitors exhibiting antiproliferative activity against non-small cell lung cancer. *J Enzyme Inhib Med Chem.* 2024;39(1):2318645.
25. Liang X, Zang J, Li X, Tang S, Huang M, Geng M, Chou CJ, Li C, Cao Y, Xu W, et al. Discovery of novel janus kinase (JAK) and histone deacetylase (HDAC) dual inhibitors for the treatment of hematological malignancies. *J Med Chem.* 2019;62(8):3898–3923.
26. Yao L, Mustafa N, Tan EC, Poulsen A, Singh P, Duong-Thi M-D, Lee JXT, Ramanujulu PM, Chng WJ, Yen JY, et al. Design and synthesis of ligand efficient dual inhibitors of janus kinase (JAK) and histone deacetylase (HDAC) based on ruxolitinib and vorinostat. *J Med Chem.* 2017;60(20):8336–8357.
27. Liang X, Tang S, Liu X, Liu Y, Xu Q, Wang X, Saidahmatov A, Li C, Wang J, Zhou Y, et al. Discovery of novel pyrrolo[2, 3-*d*] pyrimidine-based derivatives as potent jak/hdac dual inhibitors for the treatment of refractory solid tumors. *J Med Chem.* 2022;65(2):1243–1264.
28. Zeng H, Qu J, Jin N, Xu J, Lin C, Chen Y, Yang X, He X, Tang S, Lan X, et al. Feedback activation of leukemia inhibitory factor receptor limits response to histone deacetylase inhibitors in breast cancer. *Cancer Cell.* 2016;30(3):459–473.
29. Quintás-Cardama A, Kantarjian H, Cortes J, Verstovsek S. Janus kinase inhibitors for the treatment of myeloproliferative neoplasias and beyond. *Nat Rev Drug Discov.* 2011;10(2):127–140.
30. O'Shea JJ, Pesu M, Borie DC, Changelian PS. A new modality for immunosuppression: targeting the JAK/STAT pathway. *Nat Rev Drug Discov.* 2004;3(7):555–564.
31. Chen X, Zhang L, Bao Q, Meng F, Liu C, Xu R, Ji X, You Q, Jiang Z. A JAK tyrosine kinase and pseudokinase Co-inhibition strategy combines enhanced potency and on-demand activation. *Eur J Med Chem.* 2023;250:115198.
32. Shen P, Wang Y, Jia X, Xu P, Qin L, Feng X, Li Z, Qiu Z. Dual-target Janus kinase (JAK) inhibitors: Comprehensive review on the JAK-based strategies for treating solid or hematological malignancies and immune-related diseases. *Eur J Med Chem.* 2022;239:114551.
33. Changelian PS, Flanagan ME, Ball DJ, Kent CR, Magnuson KS, Martin WH, Rizzuti BJ, Sawyer PS, Perry BD, Brissette WH, et al. Prevention of organ allograft rejection by a specific Janus kinase 3 inhibitor. *Science.* 2003;302(5646):875–878.
34. Ito M, Yamazaki S, Yamagami K, Kuno M, Morita Y, Okuma K, Nakamura K, Chida N, Inami M, Inoue T, et al. A novel JAK inhibitor, peficitinib, demonstrates potent efficacy in a rat adjuvant-induced arthritis model. *J Pharmacol Sci.* 2017;133(1):25–33.
35. Pérez-Jeldres T, Tyler CJ, Boyer JD, Karuppuachamy T, Yarur A, Giles DA, Yeasmin S, Lundborg L, Sandborn WJ, Patel DR, et al. Targeting cytokine signaling and lymphocyte traffic via small molecules in inflammatory bowel disease: JAK inhibitors and S1PR agonists. *Front Pharmacol.* 2019;10:212.
36. Van Rompaey L, Galien R, van der Aar EM, Clement-Lacroix P, Nelles L, Smets B, Lepescheux L, Christophe T, Conrath K, Vandeghinste N, et al. Preclinical characterization of GLPG0634, a selective inhibitor of JAK1, for the treatment of inflammatory diseases. *J Immunol.* 2013;191(7):3568–3577.
37. Zhou J, Jiang X, He S, Jiang H, Feng F, Liu W, Qu W, Sun H. Rational design of multitarget-directed ligands: strategies and emerging paradigms. *J Med Chem.* 2019;62(20):8881–8914.
38. Wang Z, Wang M, Yang F, Nie W, Chen F, Xu J, Guan X. Multitargeted antiangiogenic tyrosine kinase inhibitors combined to chemotherapy in metastatic breast cancer: a systematic review and meta-analysis. *Eur J Clin Pharmacol.* 2014;70(5):531–538.
39. Wang S, Zhou D, Xu Z, Song J, Qian X, Lv X, Luan J. Anti-tumor drug targets analysis: current insight and future prospect. *Curr Drug Targets.* 2019;20(11):1180–1202.
40. Menet CJ, Fletcher SR, Van Lommen G, Geney R, Blanc J, Smits K, Jouannigot N, Deprez P, van der Aar EM, Clement-Lacroix P, et al. Triazolopyridines as selective JAK1 inhibitors: from hit identification to GLPG0634. *J Med Chem.* 2014;57(22):9323–9342.